Available online at www.sciencedirect.com
SCIENCE DIRECT®
Journal of Organometallic Chemistry 687 (2003) 1–11
Journal of Organometallic Chemistry
www.elsevier.com/locate/jorganchem

# The reactions of dialkyl and diarylethoxysilanes with $T_6$ silsesquioxane cages X-ray crystallographic studies of the mono-$T_6D_1$ and bis-$T_6D_2$ insertion ring expansion products

Alan R. Bassindale [a,*], Zhihua Liu [a], David J. Parker [a], Peter G. Taylor [a,*], Peter N. Horton [b], Michael B. Hursthouse [b], Mark E. Light [b]

[a] Department of Chemistry, The Open University, Walton Hall, Milton Keynes MK7 6AA, UK
[b] Department of Chemistry, University of Southampton, Highfield, Southampton SO17 1BJ, UK

Received 1 May 2003; accepted 17 June 2003

**Abstract**

Successful ring-expanding insertion reactions of $T_6$ silsesquioxane cages using dialkyl and diarylethoxysilanes have been performed to give the first reported mixed $T_6D_1$ and $T_6D_2$ silsesquioxane cages. The reactions of hexacyclohexylsilsesquioxane ($T_6$) with dialkyl and diaryldiethoxysilanes give predominantly $T_6D_2$ bis-insertion compounds while the reaction of $T_6$ with dimethylethoxysilane gives one $T_6D_1$ mono-insertion product and various $T_6D_2$ bis-insertion products as isolable components. Three of the ring-expanded products are chiral and it has been shown from their X-ray crystal structures that the pairs of enantiomers, formed as racemic mixtures, co-crystallise together. As well as comparing these structures with related ones in the literature, the possible mechanism of their formation is discussed.


*Keywords:* $T_6$ silsesquioxane cage; Alkoxysilane; Insertion reaction; Ring opening; Cage expansion; X-ray study

## 1. Introduction

Silsesquioxanes have long been of importance to those interested in modelling the chemical environment of silica surfaces on a molecular level leading to applications in catalysis, materials and surface chemistry. The challenge of developing synthetic routes to complex cages from simpler, more easily prepared ones is to develop methods of adding individual siloxane units to cages in a controlled fashion.

For example, various groups have taken trisilanol **1** (Scheme 1) and reacted it with trichlorosilanes or functionalised metal complexes to form octasilsesquioxanes (known as $T_8$'s) **2** [1–3] and metallasilsesquioxanes **3** [4,5], respectively. The only structural analogue of hexasilsesquioxanes **4** (known as $T_6$'s) that has undergone a ring expansion to date is **5**, which was formed as a by-product in Feher's synthesis of **1**. Its structure was confirmed from the X-ray crystal structure of its bis-triphenyltin analogue **6** [6]. Compound **5** itself has been found to be a useful reagent for complexing with aluminium or titanium to give heterogeneous catalysts and for reacting with siloxanes to form novel silsesquioxane–siloxane co-polymers [7–10].

While centrosymmetric $T_8$'s **2** (where R = R′) [11–16] and to a lesser extent $T_6$'s **4** [12,17] are well-established structural types in the literature, ring expansion reactions that allow them to be used directly as precursors to larger, more complex silsesquioxanes such as **5** have remained unreported until now. In this paper, we report the aqueous tetrabutylammonium fluoride (TBAF)-catalysed insertion reactions of dimethylethoxysilane or dialkyl and diaryldiethoxysilanes with hexacyclohexylsilsesquioxane ($CyT_6$) **7**. We have also examined the

* Corresponding author. Tel.: +44-1908-652512; fax: +44-1908-858327.
*E-mail address:* p.g.taylor@open.ac.uk (P.G. Taylor).

0022-328X/03/$ - see front matter © 2003 Elsevier B.V. All rights reserved.
doi:10.1016/S0022-328X(03)00622-3

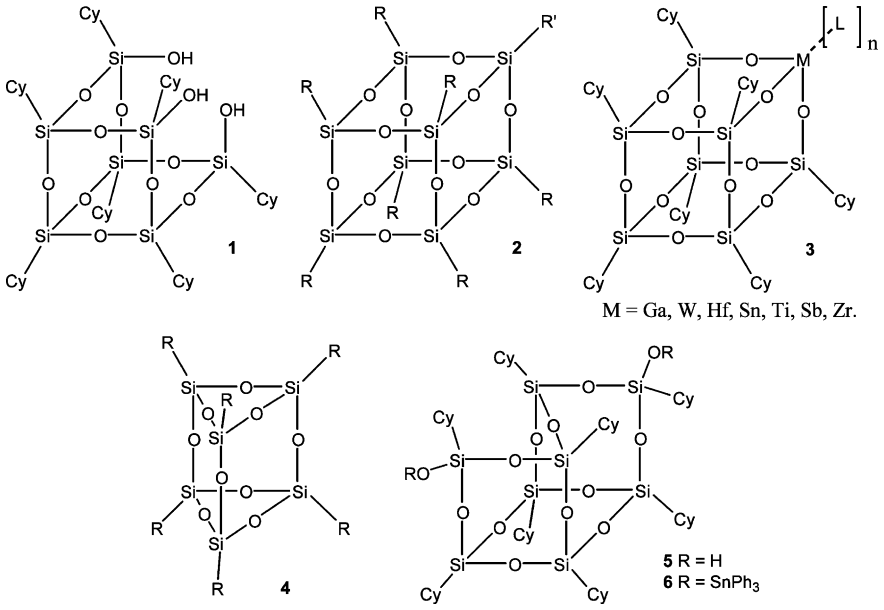


Scheme 1.

crystal structures of the compounds isolated and suggested the mechanism of their formation.

## 2. Results and discussion

The reaction of **7** with dialkyl or diaryldiethoxysilanes is described in Scheme 2. In each case, a 4:2:1 ratio of dialkoxysilane, **7** and TBAF was used, and the major products were the corresponding bis-insertion, ring-expanded $T_6D_2$ cages **8**, **9** or **10** along with a small quantity of octacyclohexylsilsesquioxane ($CyT_8$) ($<1\%$) **11** in each case.

The formation of **11** is thought to be due to TBAF-initiated rearrangement of **7** which will be discussed in a future paper [18]. Whilst the isolated yields of major products **8**, **9** and **10** are relatively low in a purely preparative sense, they are very acceptable in comparison with the typical yields reported for other silsesquioxane compounds prepared by similarly non-regioselective routes. The appearance of one D-silicon and three T-silicon peaks in the $^{29}$Si-NMR spectra with an intensity ratio 1:1:1:1 provided characteristic evidence that the bis-insertion product had been formed in each reaction. This was confirmed by obtaining single crystal X-ray structures as shown in Figs. 1 and 2

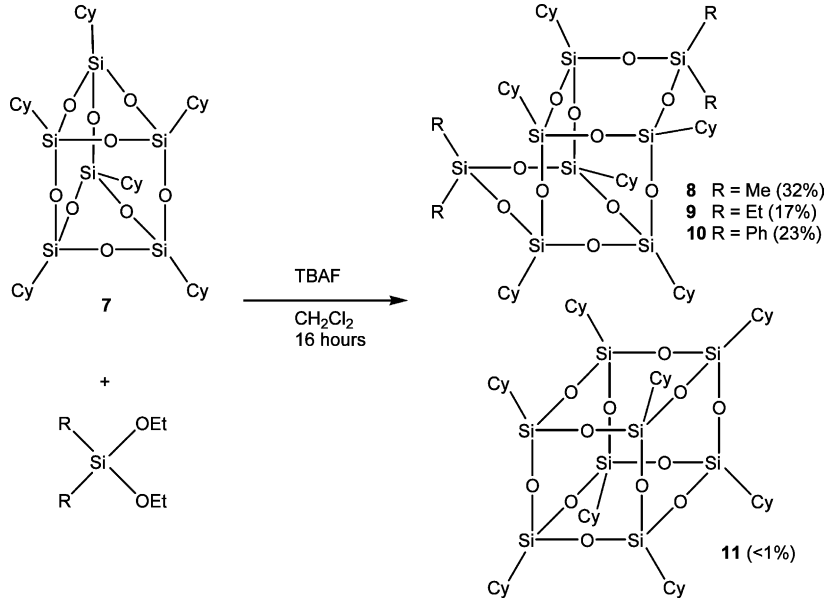


Scheme 2.

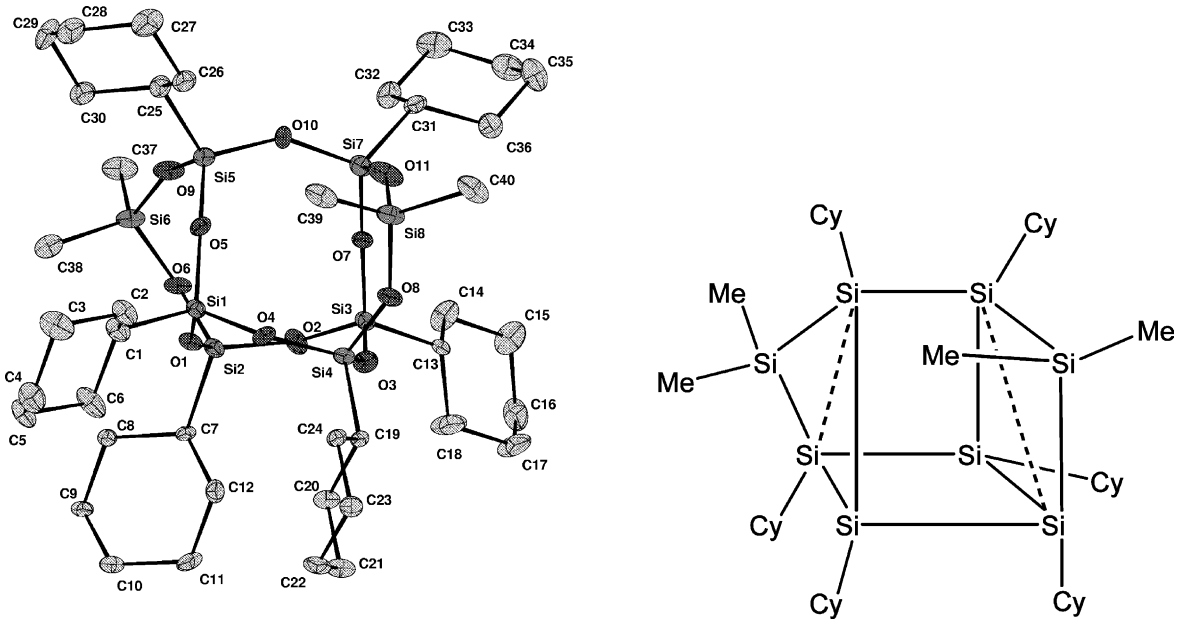


Fig. 1. ORTEP representation (left) of **8** with envelopes drawn at the 50% probability level. Selected bonding distances (Å) and bond angles (°) are given in Table 1. The simplified schematic structure (right) represents with dashed lines the edges of the former $T_6$ cage that the dimethylsiloxy groups have added across. The bridging siloxane O atoms are omitted for clarity with "Si–Si" representing the Si–O–Si moiety.

(Tables 1 and 2). Whilst the structural connectivity of **9** was confirmed by X-ray crystallography, it was not possible to obtain data of a sufficient quality for a full structural refinement of this compound.

Close inspection of the related structures **8**, **9** and **10** reveals that each is enantiomeric and that under our reaction conditions where there is no stereochemical control both enantiomers **12** and **13** will be formed as a racemic mixture. For example, the X-ray crystal structures of the two enantiomers of compound **8** are shown in Fig. 3 (Scheme 3).

The packing of molecules in each of the crystals reveals that the enantiomers co-crystallise in a 1:1 intimate array throughout the lattice. The packing of

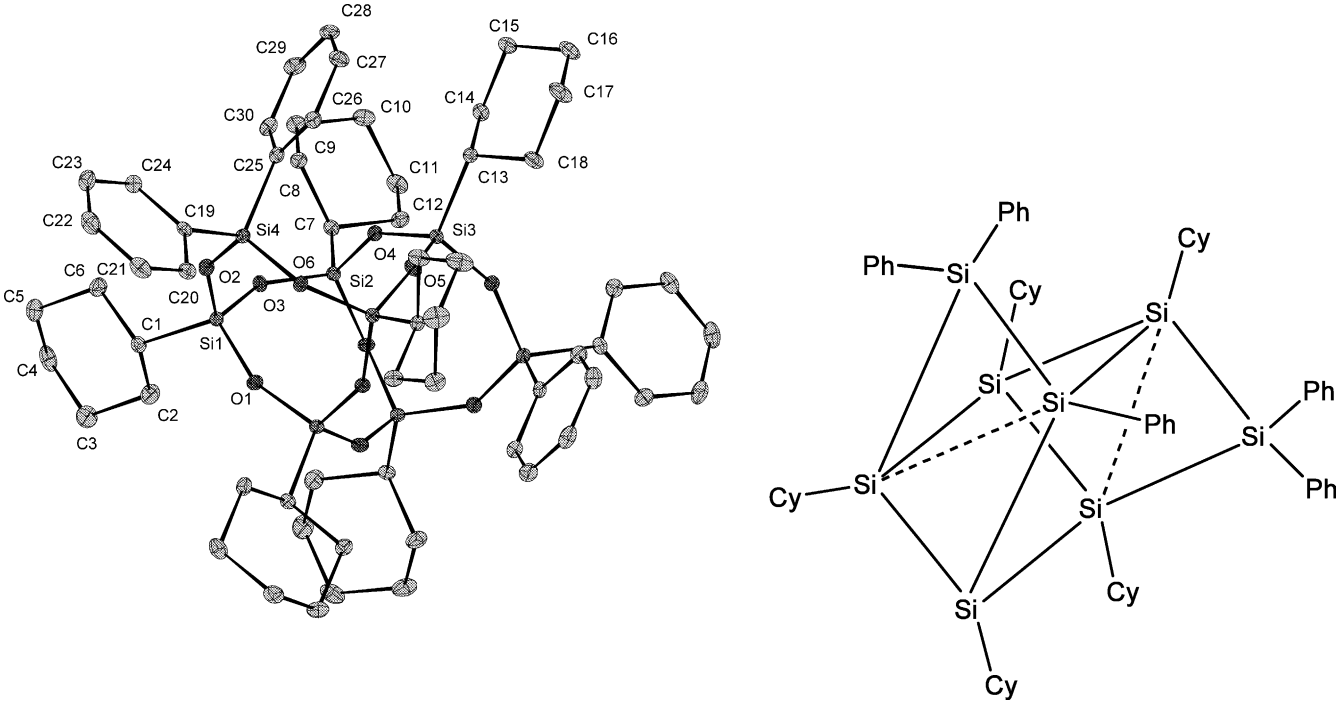


Fig. 2. ORTEP representation (left) of **10** with envelopes drawn at the 50% probability level. Selected bonding distances (Å) and bond angles (°) are given in Table 2. The simplified schematic structure (right) represents with dashed lines the edges of the former $T_6$ cage that the diphenylsiloxy groups have added across. The bridging siloxane O atoms are omitted for clarity with "Si–Si" representing the Si–O–Si moiety.

Table 1
Selected bond lengths (Å) and bond angles (°) in the crystal of **8**

| | |
|---|---|
| Si1–O4 | 1.610(5) |
| Si1–O5 | 1.615(4) |
| Si1–O1 | 1.624(5) |
| Si1–C1 | 1.839(5) |
| Si2–O2 | 1.609(5) |
| Si2–O1 | 1.625(5) |
| Si2–O6 | 1.635(5) |
| Si2–C7 | 1.861(4) |
| Si5–O10 | 1.606(5) |
| Si5–O9 | 1.610(5) |
| Si5–O5 | 1.631(5) |
| Si5–C25 | 1.847(5) |
| Si6–O9 | 1.626(5) |
| Si6–O6 | 1.629(5) |
| Si6–C38 | 1.824(8) |
| Si6–C37 | 1.853(8) |
| O4–Si1–O5 | 108.4(2) |
| O4–Si1–O1 | 110.6(2) |
| O5–Si1–O1 | 108.8(2) |
| O4–Si1–C1 | 111.6(3) |
| O5–Si1–C1 | 107.9(3) |
| O1–Si1–C1 | 109.5(2) |
| O2–Si2–O1 | 110.1(3) |
| O2–Si2–O6 | 109.7(3) |
| O1–Si2–O6 | 107.8(2) |
| O10–Si5–O9 | 108.4(3) |
| O10–Si5–O5 | 108.9(3) |
| O9–Si5–O5 | 109.9(2) |
| O10–Si5–C25 | 109.9(3) |
| O9–Si5–C25 | 110.5(3) |
| O5–Si5–C25 | 109.2(3) |
| Si1–O1–Si2 | 152.8(3) |
| Si2–O2–Si3 | 143.1(3) |
| Si5–O9–Si6 | 152.8(3) |
| Si5–O10–Si7 | 145.1(3) |
| O2–Si2–C7 | 110.0(2) |
| O1–Si2–C7 | 107.6(2) |
| O6–Si2–C7 | 111.6(2) |
| O7–Si3–O3 | 109.0(3) |
| O7–Si3–O2 | 108.1(3) |
| O3–Si3–O2 | 109.1(3) |
| O7–Si3–C13 | 113.3(2) |
| O3–Si3–C13 | 108.0(3) |
| O2–Si3–C13 | 109.2(3) |
| O9–Si6–O6 | 109.4(3) |
| O9–Si6–C38 | 108.5(3) |
| O6–Si6–C38 | 109.5(3) |
| O9–Si6–C37 | 108.3(3) |
| O6–Si6–C37 | 108.8(3) |
| C38–Si6–C37 | 112.4(4) |
| Si1–O4–Si4 | 148.2(3) |
| Si1–O5–Si5 | 150.7(3) |
| Si6–O6–Si2 | 138.1(3) |
| Si1–O1–Si2 | 152.8(3) |
| Si2–O2–Si3 | 143.1(3) |

molecules within their lattices results in each containing a considerable number of intermolecular H–H and C–H close contacts between various positions on the alkyl and aryl substituents of less than the sum of the respective pairs of van der Waals radii.

Table 2
Selected bond lengths (Å) and bond angles (°) in the crystal of **10**

| | |
|---|---|
| O1–Si1 | 1.618(2) |
| O1–Si2$^{i}$ | 1.618(2) |
| O2–Si1 | 1.622(2) |
| O2–Si4$^{i}$ | 1.632(2) |
| O3–Si1 | 1.619(2) |
| O3–Si2 | 1.620(2) |
| O4–Si3 | 1.616(2) |
| O4–Si2 | 1.621(2) |
| O5–Si3$^{i}$ | 1.609(2) |
| O5–Si3 | 1.609(2) |
| O6–Si4 | 1.620(2) |
| O6–Si3 | 1.623(2) |
| Si1–C1 | 1.844(2) |
| Si2–O1$^{i}$ | 1.618(2) |
| Si2–C7 | 1.830(2) |
| Si3–C13 | 1.834(2) |
| Si4–O2$^{i}$ | 1.632(2) |
| Si4–C19 | 1.850(2) |
| Si4–C25 | 1.853(2) |
| Si1–O1–Si2$^{i}$ | 157.53(11) |
| Si1–O2–Si4$^{i}$ | 142.28(11) |
| Si1–O3–Si2 | 144.39(10) |
| Si3–O4–Si2 | 144.61(10) |
| Si3$^{i}$–O5–Si3 | 156.79(15) |
| Si4–O6–Si3 | 147.70(10) |
| O1–Si1–O3 | 109.89(8) |
| O1–Si1–O2 | 108.98(8) |
| O3–Si1–O2 | 108.40(8) |
| O1–Si1–C1 | 109.41(9) |
| O3–Si1–C1 | 108.01(10) |
| O2–Si1–C1 | 112.13(10) |
| O1$^{i}$–Si2–O3 | 108.81(8) |
| O1$^{i}$–Si2–O4 | 109.87(8) |
| O3–Si2–O4 | 108.05(8) |
| O1$^{i}$–Si2–C7 | 110.16(10) |
| O3–Si2–C7 | 110.28(10) |
| O4–Si2–C7 | 109.64(9) |
| O5–Si3–O4 | 109.24(9) |
| O5–Si3–O6 | 109.21(6) |
| O4–Si3–O6 | 108.02(8) |
| O5–Si3–C13 | 108.21(10) |
| O4–Si3–C13 | 111.84(9) |
| O6–Si3–C13 | 110.29(10) |
| O6–Si4–O2$^{i}$ | 110.64(8) |
| O6–Si4–C19 | 105.90(9) |
| O2$^{i}$–Si4–C19 | 109.77(10) |
| O6–Si4–C25 | 110.40(10) |
| O2$^{i}$–Si4–C25 | 108.76(9) |
| C19–Si4–C25 | 111.38(10) |

A similar reaction with dimethylethoxysilane, **7** and TBAF in an 8:2:1 molar ratio gave a more complex mixture of compounds that could be separated and characterised by column chromatography (Scheme 4). As well as **11**, which was again isolated in less than 1% yield and the expected $T_6D_2$ insertion product **8** (26%), $T_6D_1$ mono-insertion product **14** (11%) and $T_6D_2$ *ortho*-bis-insertion product **15** (2%) were also obtained and structurally characterised by their single crystal X-ray structures and $^{29}$Si-NMR spectra. Structure **14** contains five silicon environments and the 1:1:1:2:2 peak intensity

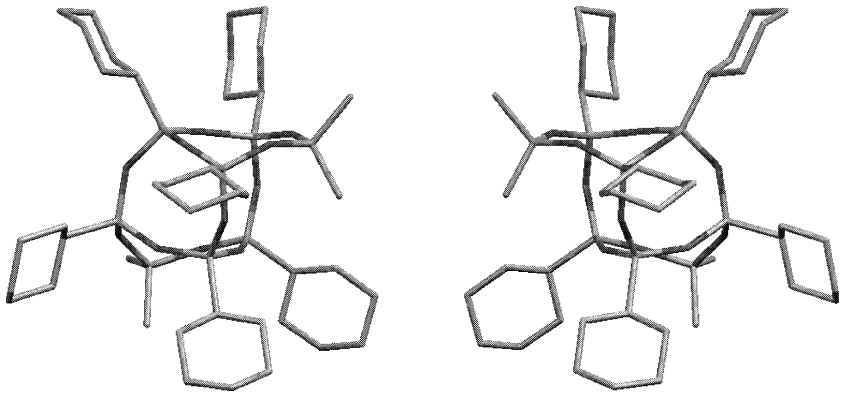

Fig. 3. The X-ray crystal structures of the enantiomers of compound **8** which correspond to the structure types **12** (left) and **13** (right), respectively. The hydrogen atoms are not shown for clarity.

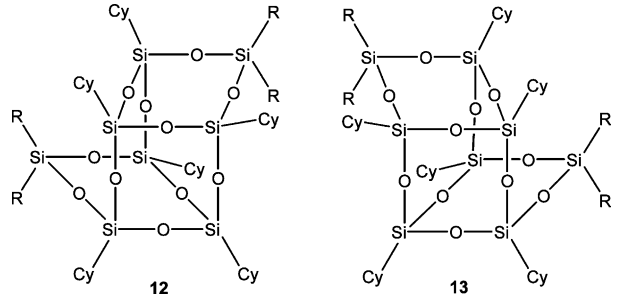

Scheme 3.

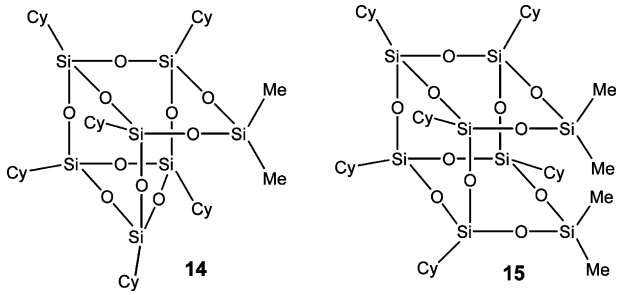

Scheme 4.

ratio in the $^{29}$Si-NMR spectrum obtained was in agreement with the X-ray structure (Fig. 4 and Table 3). The $^{29}$Si-NMR spectrum of **15** showed three peaks corresponding to each of the silicon environments with an intensity ratio 1:1:2 corresponding to the relative numbers of silicons of each type and environment. These data complement the X-ray structure for the compound (Fig. 5 and Table 4). Unlike **8**–**10**, compounds **14** and **15** are achiral. However, each crystal lattice still contains many intermolecular H–H and C–H close contact distances between the methyl and/or cyclohexyl substituents.

As compounds **8** and **10** are structurally analogous to **6**, we can compare data from their crystal structures along with those of **14**, **15** and examples of $T_6$, **16** and $T_8$, **17** cages (Scheme 5 and Table 5) from the literature [12]. By studying the mean Si–O–Si and O–Si–O bond angles in the different sized rings that comprise each cage structure a number of patterns in the data are revealed. For our purposes, we have defined an *n*-membered ring within a silsesquioxane cage as one which comprises *n* (Si–O) units. Most noticeably the mean O–Si–O bond angle is largely unaffected by changes in structure, substituents at silicon and ring size and maintains a value close to 109°, typical of a tetrahedral silicon environment. The only exception is for three-membered siloxane rings within cages, where ring strain causes a slight mean O–Si–O bond angle reduction. Ring strain also explains the smaller mean Si–O–Si bond angles in the three-membered siloxane rings compared with the four-membered siloxane rings in various cages.

With the mean O–Si–O bond angles remaining largely constant, we conclude that it is the flexibility of the Si–O–Si siloxane unit that allows different sized siloxane rings and cages to be readily formed. In Table 5, the mean Si–O–Si bond angles that have been measured vary by over 24°. For compounds **6**, **8**, **10** and **14** which contain both four- and five-membered siloxane rings, both the mean Si–O–Si and O–Si–O bond angles are unexpectedly slightly smaller in the five-membered ring than the four-membered ring when larger angles might be predicted. This may be a result of the greater conformational restrictions inherent in larger five-membered rings that reduces its degrees of freedom and constrains its geometry. Within these four compounds, increases in the mean Si–O–Si bond angles of the four-membered rings are also reflected in the conjoined five-membered rings as shown in Table 5. While compounds **6**, **8** and **10** are structurally comparable with each other, **6** has a noticeably larger average Si–O–Si bond length than **8** or **10**. This may be due to the influence of the sterically bulky triphenyltin groups

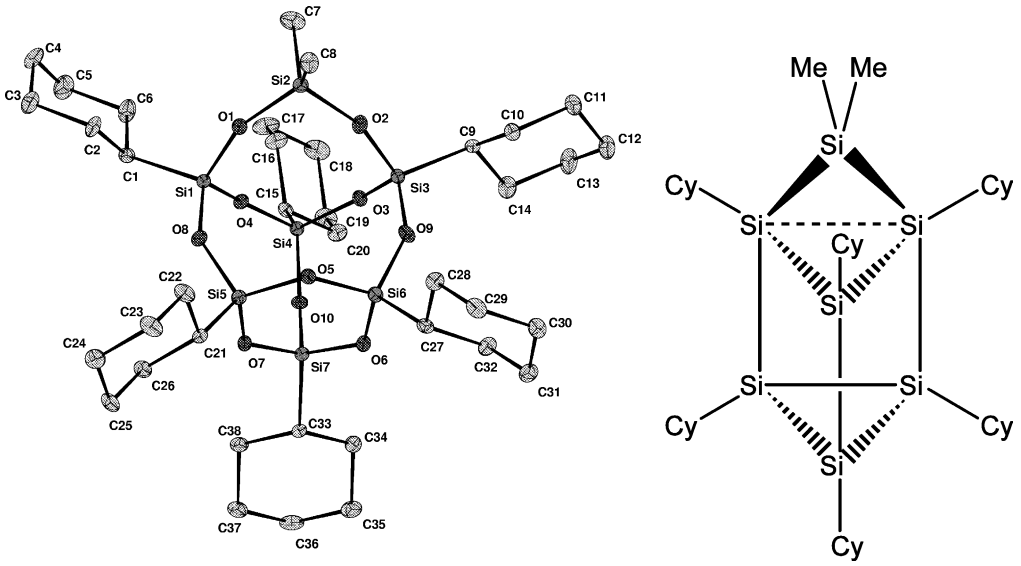


Fig. 4. ORTEP representation (left) of **14** with envelopes drawn at the 50% probability level. Selected bonding distances (Å) and bond angles (°) are given in Table 3. The simplified schematic structure (right) represents with a dashed line the edge of the former $T_6$ cage that the dimethylsiloxy group has added across. The bridging siloxane O atoms are omitted for clarity with "Si–Si" representing the Si–O–Si moiety.

causing distortion to otherwise preferred cage configuration in the crystal.

Whilst we have not studied the mechanism of these insertion reactions in detail, we envisage that the insertion occurs due to the presence of trace water via a fluoride ion-catalysed nucleophilic attack of water on the alkoxysilane on one corner silicon of the $T_6$ cage leading to an edge-opened intermediate (Fig. 6). This intermediate would then intramolecularly ring close by nucleophilic attack with loss of the alkoxide group resulting in the silane group having effectively been inserted across one $T_6$ cage edge to give a new $T_6D_1$ ring-expanded cage. The $T_6D_2$ bis- and *ortho*-bis-insertion products could then be formed by a further insertion reaction taking place across one of the edges of the remaining three-membered ring in the newly formed $T_6D_1$ cage by the attack of a further alkoxysilane molecule in a similar way. In Fig. 7, insertion of a second silane group across edge 1 would lead to the *ortho*-bis product, **15**, while insertion across edge 2 or 3 would lead to enantiomer structures **12** and **13**, respectively, in compounds **8**–**10**. In the absence of regiocontrol, edges 2 and 3 are equivalent and a racemic mixture would be obtained.

These novel $T_6D_2$ cages have a total of 10 arms, six with one functionality (based on $T_6$) and four with alternative functionalities (based on dialkoxysilane). Thus, these insertions provide a route to multifunctional cages with specific geometries that we can use to examine the interactions of arms around the cage and use as a scaffold for developing multifunctional catalysts or dendrimers.

## 3. Conclusions

We have successfully performed ring-expanding insertion reactions of $T_6$ silsesquioxane cages using dialkyl and diarylethoxysilanes to give the first reported mixed $T_6D_1$ and $T_6D_2$ silsesquioxane cages. While these reactions often lead to mixed product formation, the various components could be separated by column chromatography and characterised by multinuclear NMR spectroscopy, matrix-assisted laser desorption/ionisation (MALDI) mass spectroscopy and single crystal X-ray diffraction. The reaction of $T_6$ with dialkyl and diaryldiethoxysilanes gives predominantly a $T_6D_2$ bis-insertion compound while the reaction of $T_6$ with dimethylethoxysilane gives one $T_6D_1$ mono- and various $T_6D_2$ bis-insertion compounds as isolable components. We have postulated that the reaction's mechanism is catalysed by aqueous fluoride ion and that it is the trajectory and position of attack of the second alkoxysilane molecule on this $T_6D_1$ intermediate cage that determines which $T_6D_2$ bis-insertion compound is formed on a single molecule level.

Three of our ring-expanded products are chiral and we have shown from their crystal structures that the pairs of enantiomers formed as racemic mixtures co-crystallise together. A comparison of our crystal structure data with comparable literature compounds reveals strong similarities. In particular, we have observed that while the mean O–Si–O cage bond angle remains essentially constant from structure to structure, the mean Si–O–Si siloxane bond angle varies considerably. This is probably an important factor in explaining the variety of stable ring, ladder and cage sizes and

Table 3
Selected bond lengths (Å) and bond angles (°) in the crystal of **14**

| | |
|---|---|
| C1–Si1 | 1.842(3) |
| C7–Si2 | 1.845(3) |
| C8–Si2 | 1.841(3) |
| C15–Si4 | 1.844(3) |
| C21–Si5 | 1.843(3) |
| C33–Si7 | 1.835(3) |
| O1–Si1 | 1.612(2) |
| O1–Si2 | 1.629(2) |
| O2–Si2 | 1.623(2) |
| O3–Si4 | 1.623(2) |
| O4–Si1 | 1.618(2) |
| O4–Si4 | 1.625(2) |
| O5–Si5 | 1.638(2) |
| O6–Si7 | 1.636(2) |
| O7–Si5 | 1.636(2) |
| O7–Si7 | 1.638(2) |
| O4–Si4 | 1.625(2) |
| O5–Si5 | 1.638(2) |
| O6–Si7 | 1.636(2) |
| O7–Si5 | 1.636(2) |
| Si1–O1–Si2 | 148.70(13) |
| Si3–O2–Si2 | 156.77(14) |
| Si4–O3–Si3 | 145.05(13) |
| Si1–O4–Si4 | 158.50(13) |
| Si5–O5–Si6 | 133.29(13) |
| Si6–O6–Si7 | 128.24(12) |
| Si5–O7–Si7 | 129.29(12) |
| Si5–O8–Si1 | 139.09(12) |
| Si7–O10–Si4 | 140.63(13) |
| O1–Si1–O4 | 109.04(10) |
| O1–Si1–O8 | 108.48(11) |
| O4–Si1–O8 | 109.04(10) |
| O1–Si1–C1 | 109.63(12) |
| O4–Si1–C1 | 110.56(11) |
| O8–Si1–C1 | 110.06(11) |
| O2–Si2–O1 | 110.36(11) |
| O2–Si2–C8 | 108.32(13) |
| O1–Si2–C8 | 107.83(13) |
| O2–Si2–C7 | 108.28(14) |
| O1–Si2–C7 | 107.49(13) |
| C8–Si2–C7 | 114.55(15) |
| O3–Si4–O4 | 108.59(10) |
| O3–Si4–O10 | 109.75(10) |
| O4–Si4–O10 | 109.13(10) |
| O3–Si4–C15 | 109.61(12) |
| O4–Si4–C15 | 110.06(11) |
| O10–Si4–C15 | 109.68(12) |
| O8–Si5–O7 | 109.01(10) |
| O8–Si5–O5 | 109.71(10) |
| O7–Si5–O5 | 106.50(10) |
| O8–Si5–C21 | 108.64(12) |
| O7–Si5–C21 | 110.23(12) |
| O5–Si5–C21 | 112.69(11) |
| O10–Si7–O6 | 108.60(10) |
| O10–Si7–O7 | 108.85(10) |
| O6–Si7–O7 | 106.53(10) |
| O10–Si7–C33 | 111.13(12) |
| O6–Si7–C33 | 111.30(11) |
| O7–Si7–C33 | 110.28(12) |

structures that are known in the silsesquioxane chemistry. We are currently undertaking work on similar insertion reactions of $T_6$ cages involving dialkyl or diarylethoxysilanes with different alkyl and/or aryl groups.

## 4. Experimental

### 4.1. General

The TBAF solution in THF used contained 5% of water. Matrix-assisted laser desorption/ionisation–time of flight (MALDI–TOF) mass spectrometry studies were carried out by the University of Southampton using DBH as the matrix and dichloromethane as solvent. All NMR measurements were made on JEOL EX300 or EX400 FT instruments fitted with multinuclear probes. Spectra were recorded at 20 °C using $CDCl_3$ dried over 4 Å molecular sieves as solvent and an external reference of tetramethylsilane. Details of the X-ray crystal structure studies also undertaken by the University of Southampton can be found separately in Section 4.2.

#### 4.1.1. Synthesis of bis-insertion compounds *8*–*10* of hexacyclohexylsilsequioxane 7 from dialkyl and diaryldiethoxysilanes

In a typical reaction, **7** (0.255 g, 0.314 mmol), dialkyl or diaryldiethoxysilane (0.629 mmol) and TBAF (0.157 mmol) (0.157 $cm^3$ of a 1 M THF solution) were dissolved in dichloromethane (50 $cm^3$) and stirred at room temperature (r.t.) for 16 h. The solution was then extracted with distilled water (20 $cm^3$) and further with dichloromethane (200 $cm^3$). The organic layer was dried over anhydrous magnesium sulfate and the solvent removed under vacuum. The resulting white residue was washed with acetone (20 $cm^3$) and purified by column chromatography ($SiO_2$/hexane) to give a crystalline product **8**, **9** or **10**. Colourless crystals suitable for X-ray structure analysis were obtained by recrystallisation from a 1:1 dichloromethane–acetone solvent mixture.

##### 4.1.1.1. Bis-dimethylsilyl-hexacyclohexylsilsequioxane $T_6D_2$ insertion compound *8*.

Yield: 0.096 g (32%); $\delta_H$ (300 MHz, $CDCl_3$): 0.07 (6H, s, $CH_3$), 0.09 (6H, s, $CH_3$), 0.69 (6H, m, $CH(CH_2)_2$), 1.21 (30H, m, $CH_2$) and 1.69 (30H, m, $CH_2$); $\delta_C$ (300 MHz, $CDCl_3$): 0.00 ($SiCH_3$), 0.23 ($SiCH_3$), 23.10 ($CH(CH_2)_2$), 23.19 ($CH(CH_2)_2$), 23.43 ($CH(CH_2)_2$), 26.25 ($CH_2$), 26.31 ($CH_2$), 26.43 ($CH_2$), 26.61 ($CH_2$), 27.23 ($CH_2$) and 27.28 ($CH_2$); $\delta_{Si}$ (400 MHz, $CDCl_3$): −17.73 ($SiMe_2$), −65.95 (SiCy), −67.85 (SiCy) and −68.24 (SiCy) (1:1:1:1); *m/z* (MALDI–TOF): 959.52 [$MH^+$], 960.50, 961.48 and 962.46.

##### 4.1.1.2. Bis-diethylsilyl-hexacyclohexylsilsequioxane $T_6D_2$ insertion compound *9*.

Yield: 0.043 g (17%); $\delta_H$ (300

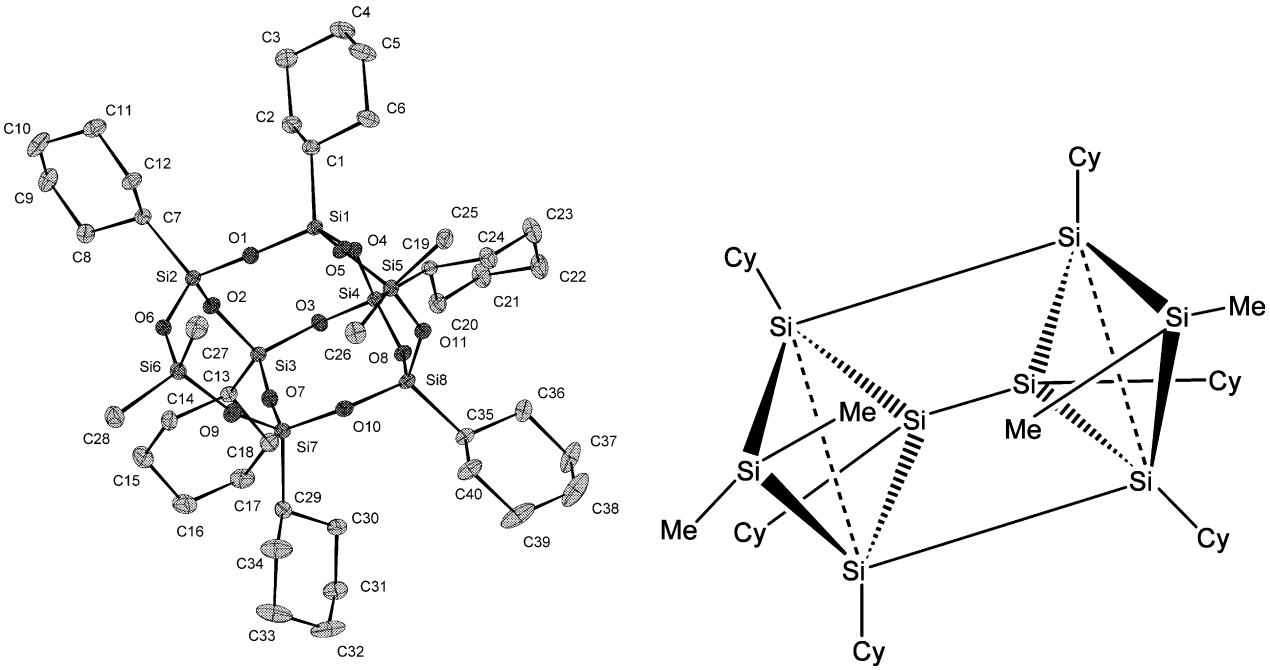


Fig. 5. ORTEP representation (left) of **15** with envelopes drawn at the 50% probability level. Selected bonding distances (Å) and bond angles (°) are given in Table 4. The simplified schematic structure (right) represents with dashed lines the edges of the former $T_6$ cage that the dimethylsiloxy groups have added across. The bridging siloxane O atoms are omitted for clarity with "Si–Si" representing the Si–O–Si moiety.

MHz, $CDCl_3$): 0.51 (8H, m, $SiCH_2$), 0.70 (6H, m, $CH(CH_2)_2$), 0.95 (12H, m, $CH_3$), 1.22 (30H, m, $CH_2$ of Cy) and 1.70 (30H, m, $CH_2$ of Cy); $\delta_C$ (300 MHz, $CDCl_3$): 6.30 ($SiCH_2$), 6.75 ($SiCH_2$), 23.41 ($CH(CH_2)_2$), 23.47 ($CH(CH_2)_2$), 23.89 ($CH(CH_2)_2$), 26.54 ($CH_2$), 26.80 ($CH_2$), 26.85 ($CH_2$), 27.48 ($CH_2$), 27.60 ($CH_2$) and 30.91 ($CH_3$); $\delta_{Si}$ (400 MHz, $CDCl_3$): −18.10 ($SiEt_2$), −66.00 (SiCy), −68.03 (SiCy) and −68.74 (SiCy) (1:1:1:1); *m/z* (MALDI–TOF): 1036.99 [M+ $Na^+$], 1038.01, 1039.03, 1040.05, 1041.07 and 1042.09.

*4.1.1.3. Bis-diphenylsilyl-hexacyclohexylsilsequioxane $T_6D_2$ insertion compound **10**.* Yield: 0.075 g (23%); $\delta_H$ (300 MHz, $CDCl_3$): 0.38 (6H, m, $CH(CH_2)_2$), 1.22 (30H, m, $CH_2$), 1.68 (30H, m, $CH_2$), 7.33 (12H, m, CH of Ph) and 7.59 (8H, m, CH of Ph); $\delta_C$ (300 MHz, $CDCl_3$): 23.33 ($CH(CH_2)_2$), 26.47 ($CH_2$), 27.42 ($CH_2$), 127.48 (CSi of Ph), 127.58 (CH of Ph), 134.02 (CH of Ph) and 134.35 (CH of Ph); $\delta_{Si}$ (400 MHz, $CDCl_3$): −46.03 ($SiPh_2$), −65.71 (SiCy), −67.70 (SiCy) and −68.00 (SiCy) (1:1:1:1); *m/z* (MALDI–TOF): 1230.78 [M+ $Na^+$].

*4.1.2. Synthesis of mono- and bis-insertion compounds (**8**, **14** and **15**) of hexacyclohexylsilsequioxane 7 from dimethylethoxysilane*

Compound **7** (0.217 g, 0.268 mmol), dimethylethoxysilane (0.112 g, 1.070 mmol) and TBAF (0.134 mmol) (0.134 $cm^3$ of a 1 M THF solution) were dissolved in dichloromethane (50 $cm^3$) and stirred at r.t. for 16 h. The solution was then extracted with distilled water (20 $cm^3$) and further with dichloromethane (200 $cm^3$). The organic layer was dried over anhydrous magnesium sulfate and the solvent removed under vacuum. The resulting white residue was washed with acetone (20 $cm^3$) and purified by column chromatography ($SiO_2$/hexane) to give three fractions **8**, **14** and **15** as white crystalline solids. Colourless crystals of each material suitable for X-ray structure analysis were obtained by recrystallisation from a 1:1 dichloromethane–acetone solvent mixture.

*4.1.2.1. Fraction 1—bis-dimethylsilyl-hexacyclohexylsilsequioxane $T_6D_2$ insertion compound **8**.* See Section 4.1.1.1 above.

*4.1.2.2. Fraction 2—mono-dimethylsilyl-hexacyclohexylsilsequioxane $T_6D_1$ insertion compound **14**.* Yield: 0.026 g (11%); $\delta_H$ (300 MHz, $CDCl_3$): 0.08 (3H, s, $CH_3$), 0.11 (3H, s, $CH_3$), 0.76 (6H, m, $CH(CH_2)_2$), 1.22 (30H, m, $CH_2$) and 1.71 (30H, m, $CH_2$); $\delta_C$ (300 MHz, $CDCl_3$): 0.00 ($SiCH_3$), 0.46 ($SiCH_3$), 22.55 ($CH(CH_2)_2$), 23.08 ($CH(CH_2)_2$), 23.33 ($CH(CH_2)_2$), 26.20 ($CH_2$), 26.31 ($CH_2$), 26.36 ($CH_2$), 26.46 ($CH_2$), 26.68 ($CH_2$), 26.73 ($CH_2$), 26.85 ($CH_2$), 27.34 ($CH_2$), 27.38 ($CH_2$), 27.47 ($CH_2$), 27.49 ($CH_2$) and 27.58 ($CH_2$); $\delta_{Si}$ (400 MHz, $CDCl_3$): −17.84 ($Me_2Si$), −56.18 (CySi of three-membered ring), −58.65 (CySi of three-membered ring), −66.76 (CySi of four-membered ring) and −67.30 (CySi of four-membered ring) (1:1:2:1:2); *m/z* (MALDI–TOF): 907.45 [M+ $Na^+$].

Table 4
Selected bond lengths (Å) and bond angles (°) in the crystal of **15**

| Molecule 1 | | Molecule 2 | |
|---|---|---|---|
| Si1–O5 | 1.611(2) | Si9–O12 | 1.609(2) |
| Si1–O1 | 1.616(2) | Si9–O16 | 1.615(2) |
| Si1–O4 | 1.621(2) | Si9–O15 | 1.627(2) |
| Si1–C1 | 1.847(3) | Si9–C41 | 1.848(3) |
| Si4–O8 | 1.621(2) | Si12–O14 | 1.619(2) |
| Si4–O4 | 1.622(2) | Si12–O15 | 1.620(2) |
| Si4–O3 | 1.630(2) | Si12–O19 | 1.621(2) |
| Si4–C19 | 1.844(3) | Si12–C59 | 1.842(3) |
| Si5–O5 | 1.633(2) | Si13–O16 | 1.618(2) |
| Si5–O11 | 1.638(2) | Si13–O22 | 1.627(2) |
| Si5–C25 | 1.834(3) | Si13–C65 | 1.835(4) |
| Si5–C26 | 1.838(3) | Si13–C66 | 1.841(4) |
| Si8–O11 | 1.623(2) | Si16–O21 | 1.617(2) |
| Si8–O8 | 1.626(2) | Si16–O22 | 1.620(2) |
| Si8–O10 | 1.627(2) | Si16–O19 | 1.623(2) |
| Si8–C35 | 1.843(3) | Si16–C75 | 1.854(3) |
| O5–Si1–O1 | 107.09(11) | O12–Si9–O16 | 108.21(12) |
| O5–Si1–O4 | 110.02(10) | O12–Si9–O15 | 108.69(11) |
| O1–Si1–O4 | 109.41(10) | O16–Si9–O15 | 109.57(11) |
| O5–Si1–C1 | 110.89(13) | O12–Si9–C41 | 110.52(12) |
| O1–Si1–C1 | 110.55(12) | O16–Si9–C41 | 109.80(13) |
| O4–Si1–C1 | 108.87(12) | O15–Si9–C41 | 110.00(12) |
| O8–Si4–O4 | 108.85(10) | O14–Si12–O15 | 109.84(10) |
| O8–Si4–O3 | 108.74(11) | O14–Si12–O19 | 108.85(11) |
| O4–Si4–O3 | 109.37(10) | O15–Si12–O19 | 108.89(11) |
| O8–Si4–C19 | 110.29(12) | O14–Si12–C59 | 110.31(12) |
| O4–Si4–C19 | 109.42(12) | O15–Si12–C59 | 107.80(12) |
| O3–Si4–C19 | 110.14(12) | O19–Si12–C59 | 111.13(12) |
| O5–Si5–O11 | 108.89(10) | O16–Si13–O22 | 109.96(11) |
| O5–Si5–C25 | 108.85(14) | O16–Si13–C65 | 108.41(16) |
| O11–Si5–C25 | 109.50(12) | O22–Si13–C65 | 108.79(16) |
| O5–Si5–C26 | 109.33(13) | O16–Si13–C66 | 107.68(16) |
| O11–Si5–C26 | 108.87(14) | O22–Si13–C66 | 109.04(14) |
| C25–Si5–C26 | 111.36(16) | C65–Si13–C66 | 112.91(15) |
| O11–Si8–O8 | 109.57(11) | O21–Si16–O22 | 107.12(11) |
| O11–Si8–O10 | 108.31(10) | O21–Si16–O19 | 110.00(11) |
| O8–Si8–O10 | 109.13(11) | O22–Si16–O19 | 109.89(11) |
| O11–Si8–C35 | 109.19(12) | O21–Si16–C75 | 110.63(13) |
| O8–Si8–C35 | 108.43(12) | O22–Si16–C75 | 110.93(12) |
| O10–Si8–C35 | 112.19(13) | O19–Si16–C75 | 108.27(12) |
| Si1–O1–Si2 | 155.91(14) | Si9–O12–Si10 | 160.49(14) |
| Si3–O3–Si4 | 136.14(13) | Si12–O14–Si11 | 146.63(13) |
| Si1–O4–Si4 | 152.62(14) | Si12–O15–Si9 | 143.24(14) |
| Si1–O5–Si5 | 148.56(13) | Si9–O16–Si13 | 146.50(14) |
| Si4–O8–Si8 | 142.46(12) | Si12–O19–Si16 | 149.44(13) |
| Si7–O10–Si8 | 144.65(13) | Si16–O21–Si15 | 153.97(14) |
| Si8–O11–Si5 | 139.99(13) | Si16–O22–Si13 | 149.42(15) |

*4.1.2.3. Fraction 3—ortho-bis-dimethylsilyl-hexacyclohexylsilsequioxane $T_6D_2$ insertion compound **15**.* Yield: 0.005 g (2%); $\delta_H$ (300 MHz, $CDCl_3$): 0.10 (12H, s, $CH_3$), 0.68 (6H, m, $CH(CH_2)_2$), 1.20 (30H, m, $CH_2$) and 1.70 (30H, m, $CH_2$); $\delta_C$ (300 MHz, $CDCl_3$): 0.00 ($SiCH_3$), 0.72 ($SiCH_3$), 23.03 ($CH(CH_2)_2$), 23.77 ($CH(CH_2)_2$), 26.47 ($CH_2$), 26.63 ($CH_2$), 26.76 ($CH_2$), 27.38 ($CH_2$), 27.45 ($CH_2$) and 29.58 ($CH_2$); $\delta_{Si}$ (400 MHz, $CDCl_3$): −18.25 ($Me_2Si$), −67.50 (CySi) and −68.94 (CySi) (1:1:2); *m/z* (MALDI–TOF): 981.7 [M + $Na^+$].

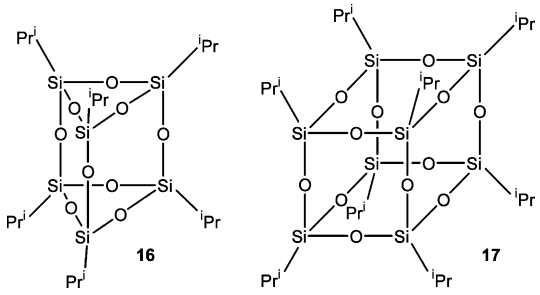


Scheme 5.

Table 5
A summary of mean Si–O–Si and O–Si–O bond angle data (°) arranged by ring size for various silsesquioxane cage compounds characterised by X-ray crystallography (one member = 1 Si–O unit)

| Compound | Bond angle type | Ring size | | |
|---|---|---|---|---|
| | | Three-membered | Four-membered | Five-membered |
| **16** | Si–O–Si | 130.4 | 134.7 | – |
| | O–Si–O | 106.4 | 108.8 | – |
| **14** | Si–O–Si | 130.3 | 144.6 | 144.5 |
| | O–Si–O | 106.5 | 109.3 | 109.2 |
| **15** | Si–O–Si | – | 147.4 | – |
| | O–Si–O | – | 109.3 | – |
| **10** | Si–O–Si | – | 149.0 | 147.2 |
| | O–Si–O | – | 109.4 | 109.1 |
| **17** | Si–O–Si | – | 149.5 | – |
| | O–Si–O | – | 108.9 | – |
| **8** | Si–O–Si | – | 149.8 | 149.6 |
| | O–Si–O | – | 109.3 | 108.8 |
| **6** | Si–O–Si | – | 154.8 | 151.5 |
| | O–Si–O | – | 109.1 | 109.0 |

### 4.2. X-ray crystallography

All structures were measured on a Nonius Kappa CCD diffractometer ($\phi$ scans and $\omega$ scans to fill asymmetric unit or Ewald sphere) using graphite monochromated Mo–$K_\alpha$ radiation ($\lambda = 0.71073$ Å). The data collection was performed in a $\psi$ rotation mode. A list of crystal data, data collection, structure solution and refinement parameters is provided in Table 6. The raw intensity data were corrected for Lorentz and polarisation effects as well as absorption correction (SORTAV) [19]. Structure solutions were searched and refined by direct methods (SHELXS 97) [20] and difference Fourier analyses (SHELXL 97) [21], respectively, based on $F^2$. Atom form factors for neutral atoms were taken from the literature [22]. Second and third row elements were allowed to refine anisotropically with hydrogen atoms assumed in idealised positions riding on their pivot atoms.

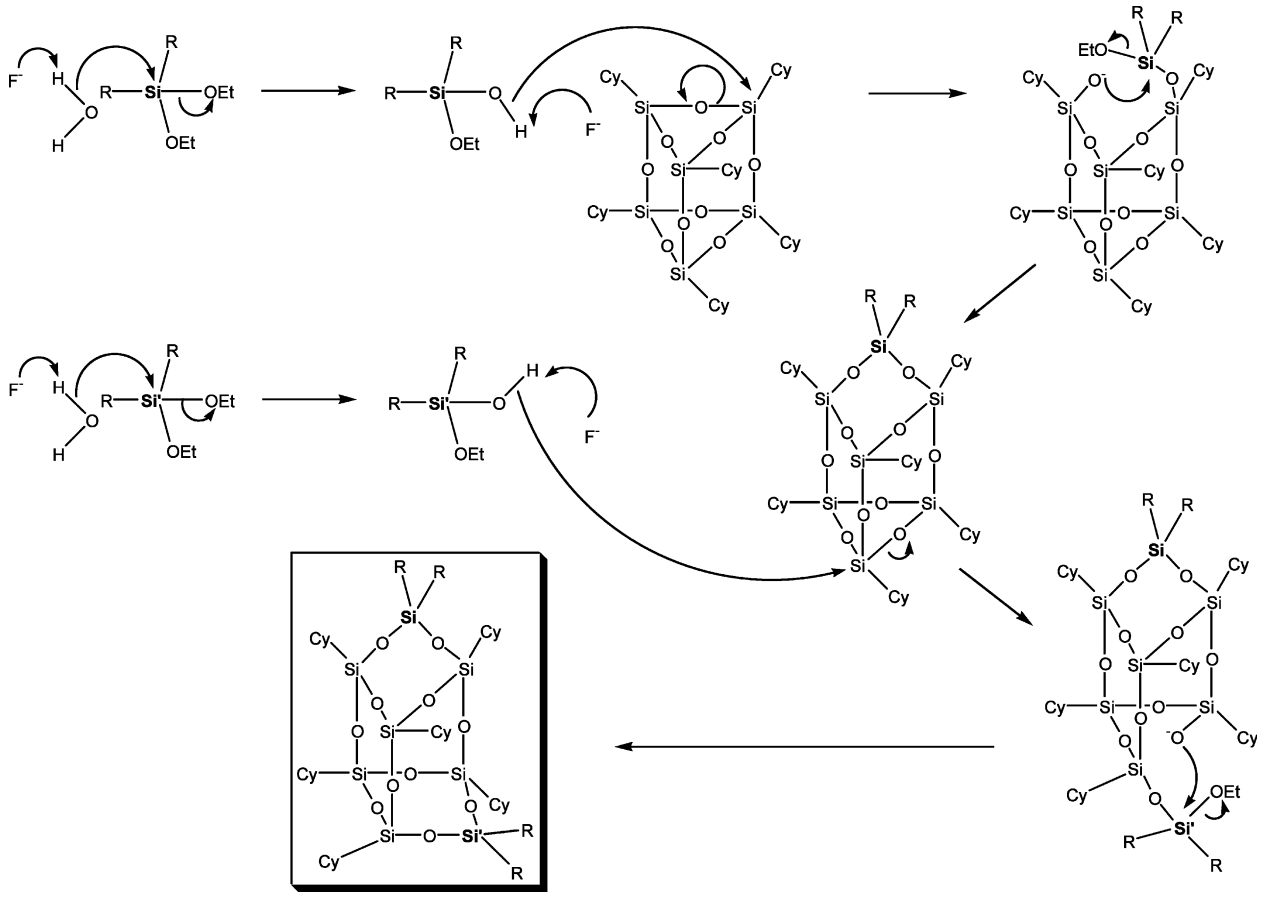

Fig. 6. A possible mechanism for silane insertion reactions into $T_6$ silsesquioxane cages catalysed by aqueous fluoride ion.

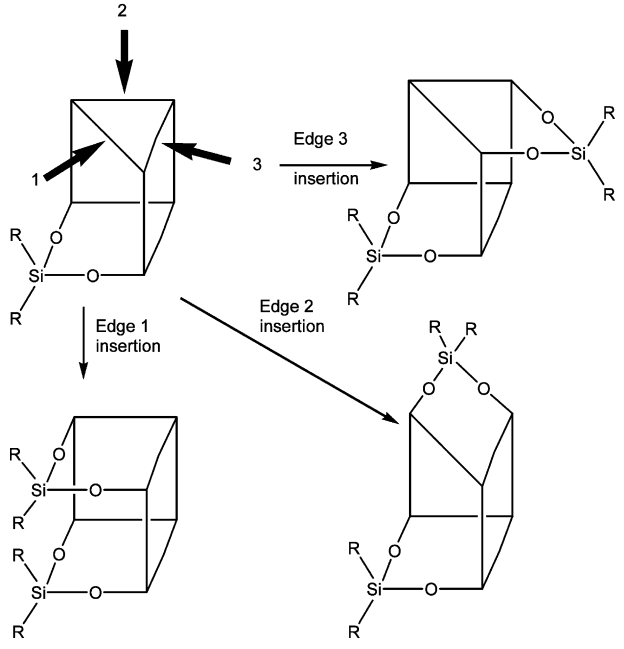


Fig. 7. The regiochemical outcomes of a second edge insertion reaction into $T_6D_1$ mono-insertion silsesquioxane cage compounds.

## 5. Supplementary material

Crystallographic data for the structures reported in this paper have been deposited with the Cambridge Crystallographic Data Centre as supplementary publication Nos. CCDC 209191–209194. Copies of the data can be obtained free of charge on application to CCDC, 12 Union Road, Cambridge, CB2 1EZ, UK (Fax: +44-1223-336033; e-mail: deposit@ccdc.cam.ac.uk or www: http://www.ccdc.cam.ac.uk).

## Acknowledgements

We would like to thank Dow Corning for their support of this work.

## References

[1] F.J. Feher, K.J. Weller, Organometallics 9 (1990) 2638.
[2] E.G. Shockey, A.G. Bolf, P.F. Jones, J.J. Schwab, K.P. Chaffee, T.S. Haddad, J.D. Lichtenhan, Appl. Organomet. Chem. 13 (1999) 311.
[3] F.J. Feher, K.J. Weller, J.J. Schwab, Organometallics 14 (1995) 2009.

Table 6
Crystal data, data collection and refinement parameters for compounds **8**, **10**, **14** and **15**

| | **8** | **10** | **14** | **15** |
|---|---|---|---|---|
| Formula | $C_{40}H_{78}O_{11}Si_8$ | $C_{60}H_{86}O_{11}Si_8$ | $C_{38}H_{70}O_{10}Si_7$ | $C_{40}H_{78}O_{11}Si_8$ |
| Molecular weight | 959.74 | 1208.01 | 883.57 | 959.74 |
| Colour | Colourless | Colourless | Colourless | Colourless |
| Morphology | Plate | Block | Block | Tablet |
| Crystal size (mm) | $0.20 \times 0.20 \times 0.05$ | $0.20 \times 0.10 \times 0.10$ | $0.20 \times 0.10 \times 0.10$ | $0.30 \times 0.20 \times 0.05$ |
| Crystal system | Triclinic | Monoclinic | Monoclinic | Triclinic |
| Space group | $P\bar{1}$ | $C2/c$ | $P2_1/n$ | $P\bar{1}$ |
| Unit cell dimensions | | | | |
| $a$ (Å) | 10.1268(5) | 19.4021(5) | 15.8472(4) | 11.203(5) |
| $b$ (Å) | 11.4163(5) | 14.5900(5) | 15.9765(4) | 21.240(5) |
| $c$ (Å) | 22.2125(13) | 24.6258(8) | 19.6690(5) | 23.033(5) |
| $\alpha$ (°) | 84.476(2) | 90 | 90 | 96.415(5) |
| $\beta$ (°) | 88.585(2) | 112.995(2) | 107.0180(10) | 97.912(5) |
| $\gamma$ (°) | 88.878(2) | 90 | 90 | 101.753(5) |
| $V$ (Å$^3$) | 2554.9(2) | 6417.1(3) | 4761.8(2) | 5259.0(3) |
| $Z$ | 2 | 4 | 4 | 4 |
| $D_{calc}$ (g cm$^{-3}$) | 1.248 | 1.250 | 1.232 | 1.212 |
| $F(0\,0\,0)$ | 1036 | 2584 | 1904 | 2072 |
| Temperature (K) | 120(2) | 120(2) | 293(2) | 120(2) |
| Reflections collected | 18225 | 17492 | 24947 | 58806 |
| Independent reflections | 8597 | 5544 | 8329 | 18125 |
| $R_{int}$ | 0.1215 | 0.0614 | 0.0793 | 0.0635 |
| $\theta$ Range (°) | 2.91–25.03 | 2.93–25.03 | 2.92–25.03 | 2.97–25.03 |
| $h$ range | −12, 12 | −23, 21 | −18, 18 | −13, 12 |
| $k$ range | −13, 13 | −17, 17 | −18, 19 | −25, 25 |
| $l$ range | −26, 26 | −29, 29 | −23, 22 | −27, 27 |
| Final $R$ indices [$F^2 > 2\sigma(F^2)$] | $R_1 = 0.0892$, $wR_2 = 0.2068$ | $R_1 = 0.0399$, $wR_2 = 0.0921$ | $R_1 = 0.0462$, $wR_2 = 0.1054$ | $R_1 = 0.0491$, $wR_2 = 0.1018$ |
| $R$ indices (all data) | $R_1 = 0.2120$, $wR_2 = 0.2547$ | $R_1 = 0.0712$, $wR_2 = 0.1038$ | $R_1 = 0.0856$, $wR_2 = 0.1189$ | $R_1 = 0.0925$, $wR_2 = 0.1163$ |
| $S$ (goodness-of-fit on $F^2$) | 1.017 | 1.037 | 0.998 | 1.008 |
| $N_{ref}$ | 8597 | 5544 | 8329 | 18125 |
| $N_{par}$ | 532 | 357 | 498 | 1071 |


[4] F.J. Feher, T.A. Budzichowski, Polyhedron 14 (1995) 3239.
[5] M. Crocker, R.H.M. Herold, A.G. Orpen, J. Chem. Soc. Chem. Commun. (1997) 2411.
[6] F.J. Feher, D.A. Newman, J.F. Walzer, J. Am. Chem. Soc. 111 (1989) 1741.
[7] J.D. Lichtenhan, N.Q. Vu, J.A. Carter, J.W. Gilman, F.J. Feher, Macromolecules 26 (1993) 2141.
[8] R.A. Mantz, P.F. Jones, K.P. Chaffee, J.D. Lichtenhan, J.W. Gilman, I.M.K. Ismail, M.J. Burmeister, Chem. Mater. 8 (1996) 1250.
[9] J.W. Gilman, D.S. Schlitzer, J.D. Lichtenhan, J. Appl. Polym. Sci. 60 (1996) 591.
[10] T.S. Haddad, J.D. Lichtenhan, Polym. Prep. 36 (1995) 511.
[11] N.V. Podberezskaya, S.A. Magarill, I.A. Baidina, S.V. Borisov, L.E. Gorsh, J. Struct. Chem. 23 (1982) 422 (English Translation).
[12] M. Unno, A. Suto, K. Takada, H. Matsumoto, Bull. Chem. Soc. Jpn. 73 (2000) 215.
[13] C. Bonhomme, P. Toledano, J. Maquet, J. Livage, L. Bonhomme-Coury, J. Chem. Soc. Dalton Trans. 9 (1997) 1617.
[14] T.N. Martynova, V.P. Korchkov, P.P. Semyannikov, J. Organomet. Chem. 258 (1983) 277.
[15] F.J. Feher, T.A. Budzichowski, J. Organomet. Chem. 373 (1989) 153.
[16] A.R. Bassindale, Z. Liu, I.A. MacKinnon, P.G. Taylor, Y. Yang, M.E. Light, P.N. Horton, M.B. Hursthouse, J. Chem. Soc. Dalton Trans., in press.
[17] H. Behbehani, B.J. Brisdon, M.F. Mahon, K.C. Molloy, J. Organomet. Chem. 469 (1994) 19.
[18] A.R. Bassindale, P.G. Taylor, Y. Yang, Personal communication.
[19] (a) R.H. Blessing, Acta Crystallogr. A 51 (1995) 33;
(b) R.H. Blessing, J. Appl. Crystallogr. 30 (1997) 421.
[20] G.M. Sheldrick, SHELXS 97_2: A Program for Crystal Structure Solution, University of Göttingen, FRG, 1998.
[21] G.M. Sheldrick, SHELXL 97_2: A Program for Crystal Structure Refinement, University of Göttingen, FRG, 1998.
[22] International Tables for Crystallography, Tables 4.2.6.8 and 6.1.1.4, Vol. C, Kluwer Academic Publishers, Dordrecht, The Netherlands, 1995.